Small-Angle X-ray Scattering Studies of Calmodulin Mutants with Deletions in the Linker Region of the Central Helix Indicate That the Linker Region Retains a Predominantly α-Helical Conformation†

Mikio Kataoka,‡,§ James F. Head,*,∥ Anthony Persechini,⊥,# Robert H. Kretsinger,⊥ and Donald M. Engelman‡

Department of Molecular Biophysics and Biochemistry, Yale University, New Haven, Connecticut 06511, Department of Physiology, Boston University School of Medicine, Boston, Massachusetts 02118, and Department of Biology, University of Virginia, Charlottesville, Virginia 22901

Received July 11, 1990; Revised Manuscript Received September 19, 1990

ABSTRACT: Two mutant forms of calmodulin were examined by small-angle X-ray scattering in solution and compared with the wild-type protein. Each mutant has deletions in the linker region of the central helix: one lacks residues Glu-83 and Glu-84 (Des2) and the other lacks residues Ser-81 through Glu-84 (Des4). The deletions change both the radii of gyration and the maximum dimensions of the molecules. In the presence of Ca^{2+}, the observed radii of gyration are 22.4 Å for wild-type bacterially expressed calmodulin, 19.5 Å for Des2 calmodulin, and 20.3 Å for Des4 calmodulin. A reduction in the radius of gyration by 1–2 Å on removal of calcium, previously observed in the native protein, was also found in the wild type and the Des4 mutant; however, no significant size change was observed in the Des2 mutant. The large calcium-dependent conformational change in calmodulin induced by the binding of melittin [Kataoka, M., Head, J. F., Seaton, B. A., & Engelman, D. M. (1989) *Proc. Natl. Acad. Sci. U.S.A. 86*, 6944–6948] was observed in all the bacterially expressed proteins. Each protein appears to undergo a transition from a dumbbell shape to a more globular conformation on binding melittin in the presence of calcium, although quantitatively the changes in the wild-type and Des4 proteins greatly exceed those in Des2. Modeling shows that the structural properties of the deletion mutants are well described by modifications of an α helix in the central linker region of the molecule. Thus, the structure of the linker region is stable enough to maintain the average orientation and separation of the lobes yet flexible enough to permit the lobes to approach each other upon binding a peptide.

Calmodulin, a ubiquitous Ca^{2+}-binding protein in eukaryotic cells, modulates various Ca^{2+}-activated processes through Ca^{2+}-dependent binding to target enzymes and structural proteins [for review, see Cohen and Klee (1988)]. The structure of calmodulin in the presence of calcium, determined by X-ray crystallography, shows the molecule to consist of two globular lobes connected by a long central helix (Babu et al., 1985, 1988; Kretsinger et al., 1986). The central helix is very unusual in that the middle portion, which we call the linker region, is apparently completely exposed to solvent. Small-angle X-ray scattering (SAXS)[1] studies have shown that the dumbbell shape is not an artifact of the crystallization conditions but also represents the conformation of the calmodulin molecule in solution near physiological ionic strength and pH (Seaton et al., 1985; Heidorn & Trewhella, 1988). These studies have also revealed a small increase in the overall length of the molecule on binding 4 equiv of Ca^{2+}.

SAXS studies of the complexes formed between calmodulin and calmodulin-binding peptides have demonstrated that the dumbbell-shaped molecule undergoes a large Ca^{2+}-dependent conformational change on binding to the peptides (Matsushima et al., 1989; Heidorn et al., 1989; Kataoka et al., 1989). Complexes with the calmodulin-binding peptide of myosin light-chain kinase and with the bee venom peptides mastoparan and melittin in the presence of calcium are globular rather than dumbbell-shaped and have a maximum dimension of near 50 Å rather than 60 Å. These studies indicate that the linker region is highly flexible, enabling the calmodulin molecule to bend and enfold the target peptide. Flexibility in the linker region is consistent with the mean crystallographic temperature factor in this region being higher than for most of the rest of the molecule (Babu et al., 1988). A bent-helix model for the calmodulin molecule in solution was proposed by Heidorn and Trewhella (1988) on the basis of small-angle X-ray scattering measurements. A bent-helix structure has also been used to model the calmodulin–peptide interaction (Persechini & Kretsinger, 1988a). In the Persechini and Kretsinger model, bending of the helix at, or near, Ser-81 enables the two lobes to be oriented in a manner such that both can interact with the α-helical target peptide. Genetically and chemically modified forms of calmodulin have also been used to show that calmodulin activation of target enzymes is dependent on the lobes being linked by a "flexible tether" (Persechini & Kretsinger, 1988b).

† This work was supported by National Institutes of Health Grants NS 20357 (J.F.H.) and GM 22778 (D.M.E.) and by National Science Foundation Grant DMB-8917285 (R.H.K.).

* To whom correspondence should be addressed.

‡ Yale University.

§ Present address: Department of Physics, Tohoku University, Aramaki, Aoba-ku, Sendai 980, Japan.

∥ Boston University School of Medicine.

⊥ University of Virginia.

Present address: Department of Physiology, University of Rochester School of Medicine and Dentistry, Rochester, NY 14642.

[1] Abbreviations: SAXS, small-angle X-ray scattering; d_{max}, maximum linear dimension; R_g, radius of gyration; WT, bacterially expressed wild-type calmodulin; Des2, bacterially expressed calmodulin in which residues Glu-83 and Glu-84 have been deleted; Des4, bacterially expressed calmodulin in which residues Ser-81, Glu-82, Glu-83, and Glu-84 have been deleted.

0006-2960/91/0430-1188$02.50/0

Persechini et al. (1989) have produced two bacterially expressed mutant forms of calmodulin with deletions in the linker region of the central helix: a two-residue deletion (Glu-83 and Glu-84, referred to as Des2) and a four-residue deletion (Ser-81, Glu-82, Glu-83, and Glu-84, referred to as Des4). In order to extend the characterization of the structural role of the central helix, we have used SAXS measurements to determine the consequences of these deletions on the solution structures of these mutant forms of calmodulin and on the complexes formed between the mutants and the bee venom peptide melittin.

Materials and Methods

Protein Preparation. Bovine brain calmodulin was prepared by the method of Masure et al. (1984). Calmodulin and deletion mutants were expressed in *Escherichia coli* and purified as described by Persechini et al. (1989). Melittin was purchased from Sigma and repurified as described previously (Kataoka et al., 1989).

Sample Preparation. Freeze-dried calmodulin preparations and melittin were dissolved in water as stock solutions. Protein concentrations were determined by quantitative amino acid analysis. Samples for X-ray scattering experiments were prepared by dialysis against the appropriate buffer, as described previously (Kataoka et al., 1989). Final dialyzed samples contained 100 mM KCl, 50 mM MOPS, 0.02% sodium azide (pH 7.4), and either 0.1 mM $CaCl_2$ or 1.0 mM EGTA. For samples containing melittin, the dialysis solution included 1.0 μM melittin.

SAXS Measurements. Most of the scattering experiments were performed on a small-angle X-ray scattering system at Yale University. A point-focused incident X-ray beam was produced by two mirrors and an Elliott GX6 generator. Scattering data were recorded on a position-sensitive detector and transferred to a VAX8800 for analysis. Analysis procedures were described previously by Kataoka et al. (1989). Data reproducibility for the wild-type and Des2 bacterially expressed forms of calmodulin were confirmed in experiments performed with the small-angle solution scattering station installed at BL10C of the Photon Factory (Tskuba, Japan) by using synchrotron radiation, as described by Ueki et al. (1985).

The small-angle X-ray scattering intensity distribution from a protein in solution is expressed by

$$I(Q) \propto \exp(-R_g^2Q^2/3)$$

where $Q = (4\pi \sin \Theta)/\lambda$ and 2Θ and λ are the scattering angle and wavelength of X-rays (Guinier & Fournet, 1955). Thus, the Guinier plot, ln $I(Q)$ vs Q^2, should approximate a straight line in the small-angle region with a slope of $-R_g^2/3$ (e.g., see Figure 2).

Scattering data were analyzed by both Guinier analysis (Guinier & Fournet, 1955) and the indirect Fourier transform method developed by Moore (1980). Since the raw data used for Guinier analysis suffered from a slit smearing effect, the results were mainly derived from the Moore analysis with a desmearing correction step, leading to slightly different values for the radii of gyration. The final data for processing were obtained by point-by-point extrapolation to zero concentration using a series of scattering curves at different protein concentrations in the range of 3–30 mg/mL.

Model Building. Molecular modeling for Des2 and Des4 mutants was performed on the Evans and Sutherland PS360 Graphics system using the program INSIGHT (Insight molecular modeling system, Biosym Technologies, San Diego, CA), starting from the crystal structure coordinates of calmodulin in the Brookhaven Data Bank (3CLN.PDB; Babu et al., 1988). The fragment Ile-85–Ala-147 was created and connected to the fragments Thr-5–Glu-82 or Thr-5–Asp-80, minimizing the deviation of the peptide backbone of the central helix. In building these models, we assumed explicitly that the entire central helix retains a helical conformation and that each fragment retains its original structure. Thus, each model has a helical segment from Phe-65 to Phe-92 or the equivalent position.

A distance distribution function, $p(r)$, was calculated for each model, as the histogram of the distances between all pairs of atoms in the molecule. The radius of gyration, R_g^{calc} (Table II), of each model was derived as

$$R_g^2 = \sum r^2p(r)/\sum p(r)$$

The d_{max}^{calc} value shown in Table II is the largest interatomic distance in the model.

Table I: Structural Parameters Obtained by SAXS Measurements[a]

	R_g (Guinier)	R_g (Moore)	d_{max}[b]	D
Wild-Type Calmodulin				
−melittin				
$-Ca^{2+}$	19.4 (0.1)	20.5 (0.1)	57.5	27.9 (0.7)
$+Ca^{2+}$	20.0 (0.2)	22.4 (0.2)	62.5	33.8 (1.6)
+melittin				
$-Ca^{2+}$	19.8 (0.2)	20.5 (0.1)	60.0	
$+Ca^{2+}$	18.2 (0.2)	17.8 (0.2)	47.5	
Des2 Mutant Calmodulin				
−melittin				
$-Ca^{2+}$	19.0 (0.3)	19.2 (0.2)	52.5	24.0 (1.1)
$+Ca^{2+}$	18.8 (0.4)	19.5 (0.4)	52.5	25.6 (3.1)
+melittin				
$-Ca^{2+}$	19.0 (0.3)	19.5 (0.2)	52.5	
$+Ca^{2+}$	18.4 (0.2)	18.0 (0.2)	47.5	
Des4 Mutant Calmodulin				
−melittin				
$-Ca^{2+}$	18.8 (0.1)	19.4 (0.1)	52.5	24.6 (0.8)
$+Ca^{2+}$	19.3 (0.1)	20.3 (0.1)	57.5	28.0 (1.6)
+melittin				
$-Ca^{2+}$	19.3 (0.2)	19.6 (0.1)	57.5	
$+Ca^{2+}$	17.3 (0.2)	17.1 (0.1)	45.0	
Control (Bovine Brain Calmodulin)[c]				
−melittin				
$-Ca^{2+}$	19.5 (0.1)	20.3 (0.1)	57.5	27.4 (0.8)
$+Ca^{2+}$	20.2 (0.2)	22.6 (0.3)	62.5	34.3 (1.7)
+melittin				
$-Ca^{2+}$	20.9 (0.2)	22.5 (0.2)	60.0	
$+Ca^{2+}$	18.0 (0.2)	17.9 (0.1)	47.5	

[a] Data are shown in angstroms with errors in parentheses. [b] Error in each value is 2.5 Å. [c] Data taken from Kataoka et al. (1989).

Results and Discussion

Bacterially Expressed "Wild-Type" Calmodulin. Prior to making measurements on mutant forms of calmodulin, we compared the solution structure of the wild type calmodulin expressed in E. coli (bacterial calmodulin) with that of bovine brain calmodulin. The bacterial calmodulin lacks the post translational trimethylation of Lys-115 and the N-acetylation found in the native protein. However, as shown in Table I, the structural parameters of these proteins are essentially identical. No significant differences in the scattering functions and the derived distance distribution functions, $p(r)$, were seen. The apparent radius of gyration (R_g) of the bacterial calmodulin shows a normal concentration dependence (Figure 1). In the presence of calcium the concentration dependence is indistinguishable from that of the bovine brain protein, although in the presence of EGTA, the slope for bovine cal-

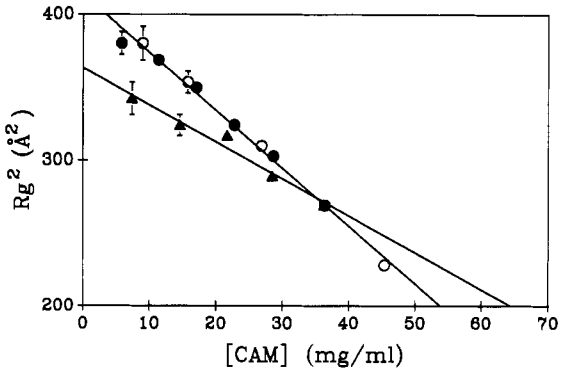

FIGURE 1: Concentration dependence of R_g for bacterially expressed wild-type calmodulin [with Ca^{2+} (●) and without Ca^{2+} (▲)] and bovine brain calmodulin [with Ca^{2+} (○)].

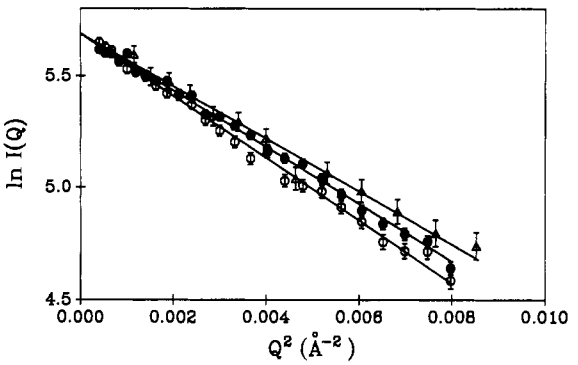

FIGURE 2: SAXS data for bacterially expressed forms of calmodulin [wild type (○), Des2 (△), and Des4 (●)] in the form of Guinier plots. For the benefit of comparison of the gradients, the $I(0)$ for each protein has been adjusted to the same value. See Materials and Methods for the derivation of R_g from such plots.

modulin is steeper [cf. Figure 2, Seaton et al. (1985)]. In principle, the concentration dependence of R_g determined by SAXS is dependent on interparticle interference, in the absence of aggregation. As seen in Figure 1, bovine brain calmodulin gives a smaller R_g value for higher protein concentrations (Seaton et al., 1985; Heidorn & Trewhella, 1988). Interparticle interference of this type is mainly due to an excluded volume effect and not electrostatic interactions (Guinier & Fournet, 1955). The strong interparticle interference observed with calmodulin appears to be a consequence of its unusual dumbbell shape. Differences in the concentration dependence of R_g between bacterial wild-type and native calmodulin would not be expected despite the differences in posttranslational modifications. The reason for the steeper slope for bovine calmodulin in the absence of calcium is not clear.

In bovine brain calmodulin, Ca^{2+} binding induces an increase in R_g of 1–2 Å and in maximum dimension (d_{max}) of about 4 Å (Seaton et al., 1985), while melittin binding in the presence of Ca^{2+} induces a decrease in both values (Kataoka et al., 1989). Bacterial wild-type calmodulin shows the same behavior on binding Ca^{2+} and melittin (Table I). Since our results show no difference between the bacterial wild-type calmodulin and the bovine brain protein, in terms of solution scattering, we will hereafter compare the structures of the mutant forms of calmodulin only with that of the wild type.

Bacterially Expressed Forms of Calmodulin. Initially we investigated the structures of the proteins in the presence of Ca^{2+}, since the crystal structure of the native protein in this form is known. Figure 2 shows Guinier plots of wild-type calmodulin, Des2, and Des4 in the presence of Ca^{2+}. All plots show straight-line relationships; however, small but distinct differences in the slopes of the three curves are seen, reflecting

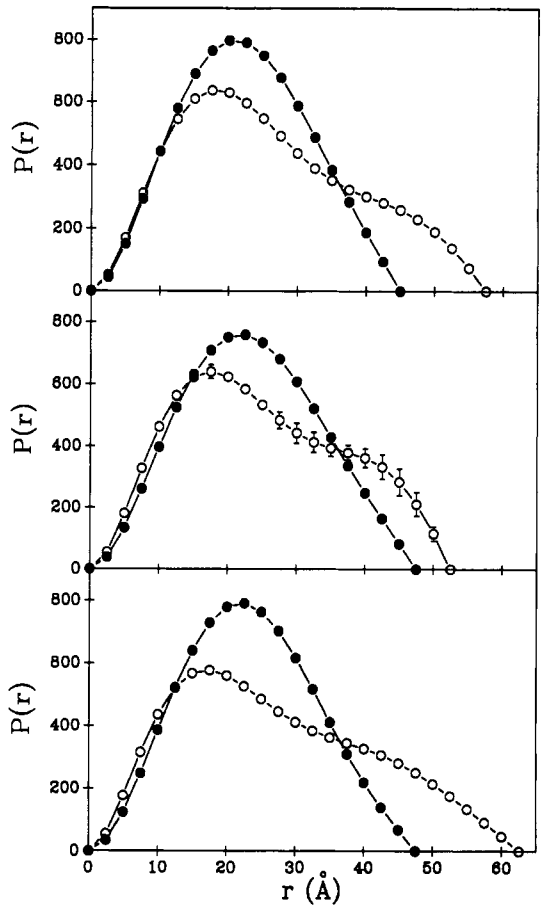

FIGURE 3: Distance distribution functions, $p(r)$, for bacterially expressed forms of calmodulin: (bottom) wild type, (middle) Des2, and (top) Des4, with Ca^{2+} (○) and with Ca^{2+} and melittin (●). All data points include error bars; however, in most cases these are within the symbol used to indicate the data point.

differences in the radii of gyration. The distance distribution functions, $p(r)$, for these three forms of calmodulin are shown in Figure 3 (open circles). The first peak principally represents interatomic distances within each lobe of the molecule, while interlobe distances are represented by the shoulder. The shapes of the $p(r)$ curves indicate that each protein exists in a dumbbell-like shape in solution, while the maximum dimension (d_{max}) varies. [The d_{max} is defined as the point where $p(r)$ converges to zero.] The values are summarized in Table I.

The R_g of a dumbbell-shaped molecule can be expressed by using the radius of gyration of the globular lobes, R_g(dom), and the center to center distance between the two lobes, D, as

$$R_g^2 = R_g(\text{dom})^2 + D^2/4$$

(Fujisawa et al., 1987). The width and position of the first peak in the $p(r)$ function is similar for all three forms of calmodulin, indicating that the size and shape of each lobe, and hence R_g(dom), is not changed significantly by the deletions. Observed changes in R_g therefore result from changes in D. A value for R_g(dom) can be derived from the initial slope of the ln $(I(Q)/Q)$ vs Q^2 plot (Fujisawa et al., 1987). For bovine brain calmodulin, R_g(dom) = 15.0 ± 0.2 Å in the absence of Ca^{2+} and 14.7 ± 0.6 Å in the presence of Ca^{2+}, taking the radii of the two lobes in each molecule as being equal (Kataoka et al., 1989). On the basis of these values and the R_g values determined in this study, values for D have been calculated for each structure from the above relationship (Table I). The value for D decreases from 34 Å for the wild type to 26 Å for Des2 and to 28 Å for Des4. The observed

Table II: Structural Parameters Calculated from Model Structures

sample	R_g^{calc} (Å)	R_g^{obs} (Å)	d_{max}^{calc} (Å)	d_{max}^{obs} (Å)
wild type	21.6	22.4	68	62.5
Des2	19.4	19.5	57	52.5
Des4	20.3	20.3	64	57.5

maximum dimension of the molecule (d_{max}) decreases by 10 Å for Des2 and 5 Å for Des4. If the central helix remains as an α-helix in solution, the deletion of a single residue would be expected to cause a decrease in the helix length of 1.5 Å. The decrease in Des4 would therefore be expected to be 6 Å, close to the observed decrease of 5 Å. However, the measured decrease for Des2, 10 Å, is much greater than the 3 Å expected from the shortening of the helix alone, indicating that an additional factor(s) must be taken into account. The other major consideration appears to be the relative orientation of the lobes.

In the crystal structure of the native form of calmodulin, the lobes of the dumbbell are not positioned symmetrically on the axis of the central helix (Babu et al. 1985, 1988; Kretsinger et al. 1986). Rather, the center of each lobe is displaced significantly from the axis. In the native protein the displacements of the two lobes are oriented trans with respect to one another. Assuming the central helix retains its helicity in free solution, then the removal of a single residue from the helix would be expected to result in the relative rotation of the lobes by approximately 100° (as well as moving 1.5 Å closer). In the Des2 mutant, the lobes, displaced by almost 200°, would therefore be nearly cis with respect to one another, while the Des4 mutant, displaced by 400°, would once again be close to the trans configuration. Changes in the value of D, calculated from the observed R_g values, are therefore not solely related to changes in the length of the linker region but also to the relative angular displacement of the two lobes.

Figure 4 shows the model structures of the deletion mutants, generated with the assumptions that the linker region remains α-helical and the rest of the molecule remains as in the crystal structure. The calculated parameters R_g and d_{max} for these models are given in Table II. The R_g values and the size order, WT > Des4 > Des2, are well explained by the models; however, there are discrepancies between the calculated and observed d_{max} values. Such differences in native calmodulin have been interpreted as representing differences between the crystal and solution structures of the protein (Heidorn & Trewhella, 1988). However, the calculation of a solution scattering profile based on the crystal structure is not necessarily straightforward and not without ambiguities (Pickover & Engelman, 1982; Lattman, 1989). Differences between observed and calculated values may therefore also be attributable in part to the limitations of the calculations.

Effect of Ca^{2+} Binding. Ca^{2+} removal from calmodulin by EGTA causes a decrease in R_g and d_{max} of the molecule that is consistent with a net movement of the lobes of the molecule toward one another (Seaton et al., 1985). Similar changes of R_g and d_{max} are observed with the Des4 mutant calmodulin; however, there is little Ca^{2+} effect observed for Des2. This result indicates that the inward displacement of the lobes may occur in an uninhibited fashion when the lobes are oriented in a trans configuration, even with the central helix shortened by 6 Å, as in Des4. When the lobes are in the proposed cis orientation, as in Des2, the inward displacement may either be inhibited or result in a twisting of the helix that results in little or no net change in R_g and d_{max}. The relative orientation of the lobes may therefore have an important influence on the structural transitions available to the molecule, although they

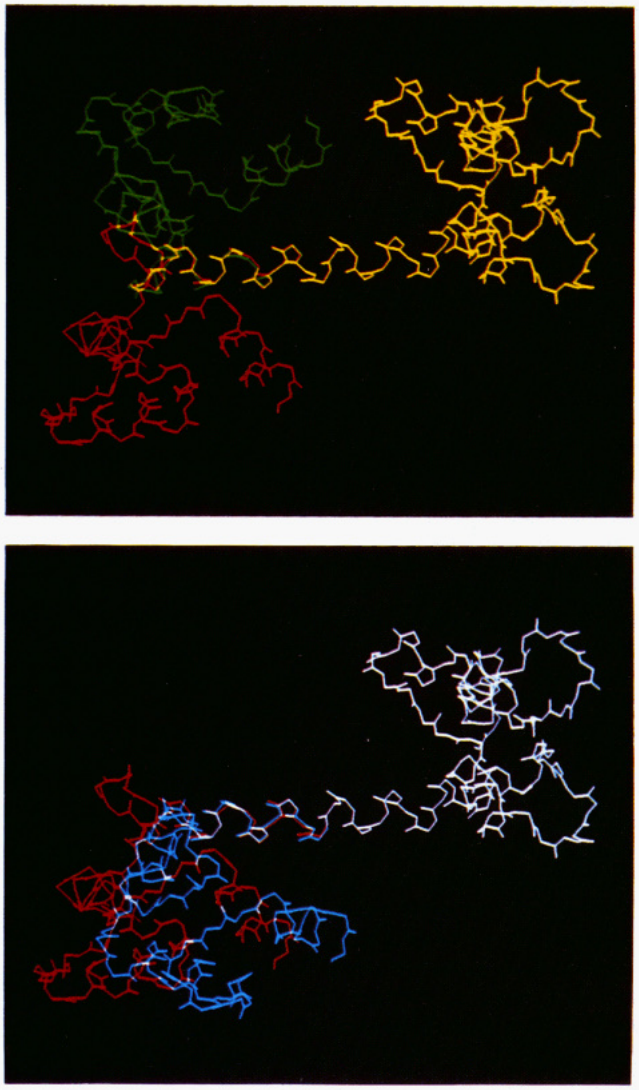

FIGURE 4: Model structures of deletion mutants of calmodulin compared with wild type. (Top) Des2 (green) and wild type (red). (Bottom) Des4 (blue) and wild type (red). Yellow and white represent the common structure between the wild type and mutant.

appear to have little effect on the ability of the protein to activate target enzymes (Persechini et al., 1989).

Effect of Melittin Binding. Our previous SAXS studies showed that calmodulin undergoes a large, Ca^{2+}-dependent conformational change on binding to the bee venom peptide melittin (Kataoka et al., 1989). Persechini et al. (1989) showed that the deletion mutants retain the ability to bind to melittin and to a calmodulin-binding peptide from myosin light-chain kinase (M-13). SAXS measurements of the complexes between melittin and the bacterially expressed forms of calmodulin show that calcium-dependent conformational changes occur that are similar to those observed for the native protein. The $p(r)$ functions consist of a single peak with a maximum near 22 Å and no shoulder, indicating the formation of a complex with an overall globular shape for all three (Figure 3, solid circles). The maximum dimension of the complexes for the mutants are ordered WT = Des2 (47.5 Å) > Des4 (45 Å). However, the *changes* in the R_g and d_{max} values of each molecule on binding melittin are ordered WT > Des4 $\gg$ Des2. In the absence of calcium, a dumbbell shape is maintained in all cases.

Persechini and Kretsinger (1988a) proposed a model for the calmodulin–peptide complex in which the central helix becomes bent, twisting the two lobes into a cis configuration while

bringing one lobe on either side of the target peptide. The large decreases seen in R_g and d_{max} for WT and Des4 can be attributed to the trans to cis conformational change accompanied by the bending to enfold the target. For the Des2 mutant, which is already in the cis configuration, the changes in R_g and d_{max} are far smaller. The present results are therefore consistent with the model of Persechini and Kretsinger (1988a).

The results of these SAXS studies of the mutant forms of calmodulin indicate that the linker region retains an α-helical conformation in solution. When two and four residues are deleted in this region, there is a relative rotation of the lobes as a turn of the helix is removed. In the presence of melittin [and apparently mastoparan (Matsushima et al., 1989) and M-13 (Heidorn et al., 1989)], the calmodulin linker region becomes bent, bringing the lobes of the molecule into cis apposition to bind to the target peptide. For WT and Des4, this requires a transition from the trans conformation, while for Des2, a small bend alone would permit "chelation" of the target.

SAXS measurements give a time-averaged structure of molecules in solution. The structures described, based on the results obtained in this study, represent models of this time-averaged structure. Other conformations of calmodulin will exist, as part of a dynamic exploration of three-dimensional space by the molcule. Some states, even with low occupancy, may represent essential steps in the pathways of folding and interaction. However, our models show that the properties of the deletion mutants are consistent with modifications of a linker region in the central helix that predominantly exists as an α helix. Thus, the linker region is sufficiently stable to maintain the average orientation and separation of the lobes yet sufficiently flexible to permit the lobes to approach each other on binding a peptide.

ACKNOWLEDGMENTS

We thank T. Kahn for his help on molecular modeling. Thanks are also due to Y. Inoko and K. Kobayashi for their help in experiments at the Photon Factory, Tskuba, Japan. SAXS measurements at the Photon Factory were performed under the approval of the Photon Factory Program Advisory Committee (Proposal No. 90-060).

Registry No. Ca^{2+}, 7440-70-2; melittin, 20449-79-0.

REFERENCES

Babu, Y. S., Sack, J. S., Greenhough, T. J., Bugg, C. E., Means, A. R., & Cook, W. J. (1985) *Nature 315*, 37–40.

Babu, Y. S., Bugg, C. E., & Cook, W. J. (1988) *J. Mol. Biol. 204*, 191–204.

Cohen, P., & Klee, C. B., Eds. (1988) *Calmodulin.* Molecular Aspects of Cellular Regulation, Vol. 5, Elsevier Biomedical Press, Amsterdam.

Fujisawa, T., Ueki, T., Inoko, Y., & Kataoka, M. (1987) *J. Appl. Crystallogr. 20*, 349–355.

Guinier, A., & Fournet, G. (1955) in *Small-angle Scattering of X-rays*, J. Wiley, New York.

Heidorn, D. B., & Trewhella, J. (1988) *Biochemistry 27*, 909–915.

Heidorn, D. B., Seeger, P. A., Rokop, S. E., Blumenthal, D. K., Means, A. R., Crespi, H., & Trewhella, J. (1989) *Biochemistry 28*, 6757–6764.

Kataoka, M., Head, J. F., Seaton, B. A., & Engelman, D. M. (1989) *Proc. Natl. Acad. Sci. U.S.A. 86*, 6944–6948.

Kretsinger, R. H., Rudnick, S. E., & Weissman, L. J. (1986) *J. Inorg. Biochem. 28*, 289–302.

Lattman, E. (1989) *Proteins: Struct., Funct., Genet. 4*, 149–155.

Masure, H. R., Head, J. F., & Tice, H. (1984) *Biochem. J. 218*, 691–696.

Matsushima, N., Izumi, Y., Matsuo, T., Yoshino, H., Ueki, T., & Miyake, Y. (1989) *J. Biochem. (Tokyo) 105*, 883–887.

Moore, P. B. (1980) *J. Appl. Crystallogr. 13*, 168–175.

Persechini, A., & Kretsinger, R. H. (1988a) *J. Cardiovasc. Pharmacol. 12* (Suppl. 5), S1–S12.

Persechini, A., & Kretsinger, R. H. (1988b) *J. Biol. Chem. 263*, 12175–12178.

Persechini, A., Blumenthal, D. K., Jarret, H. W., Klee, C. B., Hardy, D. O., & Kretsinger, R. H. (1989) *J. Biol. Chem. 264*, 8052–8058.

Pickover, C. A., & Engelman, D. M. (1982) *Biopolymers 21*, 817–831.

Seaton, B. A., Head, J. F., Engelman, D. M., & Richards, F. M. (1985) *Biochemistry 24*, 6740–6743.

Ueki, T., Hiragi, Y., Kataoka, M., Inoko, Y., Amemiya, Y., Izumi, Y., Tagawa, H., & Muroga, Y. (1985) *Biophys. Chem. 23*, 115–124.